Research Article

Jianxi Li#, Shuya Zhang#, Yaqin Fan, Aosong Wang, Zhuang Miao, Peng Cheng, and Hanzhou Liu*

Effect of phenyltrimethoxysilane coupling agent (A153) on simultaneously improving mechanical, electrical, and processing properties of ultra-high-filled polypropylene composites

https://doi.org/10.1515/epoly-2022-0056
received May 19, 2022; accepted June 08, 2022

Abstract: The improvement of mechanical properties, electrical properties, and processing properties of ultra-high-filled thermal insulation polypropylene (PP) composites has been plagued by high filling amount of heat-conducting fillers such as alumina powder (Al_2O_3) and expanded graphite. In order to improve its properties, this article uses a high-temperature-resistant coupling agent (A153) to modify the PP composite. The results of this study show that when the content of A153 reaches 7.5 phr, the tensile strength of PP composite can reach 5 MPa, the elongation at break can reach 25%, and the volume resistivity can reach 12.8×10^{12} Ω·m, and the maximum thermal conductivity is 1.82 $W \cdot m^{-1} \cdot K^{-1}$. The processability also shows that the introduction of A153 can increase the melt flow rate and effectively improve the processability of the material.

Keywords: ultra-high filling, polypropylene, thermal conductivity, mechanical properties, processability

1 Introduction

With the development of science and technology, the requirements for the thermal conductivity of materials in the fields of microelectronic packaging, automobile, aerospace, electrical insulation, and so on are becoming higher and higher, especially the electronic components, which have high-precision, high integration, and high power, but the volume has gradually become smaller, which leads to a large amount of heat gathering in a narrow space and cannot be dissipated (1,2). If the heat is not dissipated on time, the continuous high temperature will overload or even fail the electronic components, which will shorten the service life of the electronic components and may cause serious harm. In order to ensure the continuous and efficient operation of electronic components, effective heat transfer and heat dissipation have become urgent problems to be solved (3–5). Therefore, the direct contact between high thermal conductivity polymer materials and electronic components to realize heat transfer has attracted extensive attention.

Polymers have the advantages of excellent electrical insulation, good processing performance, high chemical stability, and low cost. They are very suitable as the base material of thermal conductive materials (6). However, the thermal conductivity of common polymer materials is poor, and the thermal conductivity coefficient is generally lower than 0.2 $W \cdot m^{-1} \cdot K^{-1}$ (7,8). Adding ceramic, metal, and carbon materials with excellent heat conductivity to the polymer can effectively improve the thermal conductivity of the material. There is no doubt that the thermal conductivity of thermal conductive fillers is an important factor affecting the thermal conductivity of composites. In addition, the shape of the filler will also have an important impact on thermal conductivity. Weidenfeller and Kirchberg (9) studied the thermal conductivity of PP

# These authors contributed equally to this work.

* **Corresponding author: Hanzhou Liu,** State Key Laboratory of Radiation Medicine and Protection, School of Radiation Medicine and Protection, Soochow University, Suzhou 215123, China, e-mail: hzhliu@suda.edu.cn
Jianxi Li, Yaqin Fan, Zhuang Miao, Peng Cheng: CGN Advanced Materials Technology (Suzhou) Co., Ltd., Taicang 215400, China
Shuya Zhang: State Key Laboratory of Radiation Medicine and Protection, School of Radiation Medicine and Protection, Soochow University, Suzhou 215123, China
Aosong Wang: China Nuclear Power Engineering Co., Ltd., Shenzhen 518000, China

filled with Fe_3O_4, glass fiber, talc powder, and copper powder. It was found that when the volume fraction of filler reached 30%, the thermal conductivity of PP/TAIC powder composite could be as high as 2.5 $W{\cdot}m^{-1}{\cdot}K^{-1}$, which was significantly higher than that of PP/copper powder composite, which was 1.25 $W{\cdot}m^{-1}{\cdot}K^{-1}$, while the thermal conductivity of copper was about 40 times that of talc powder. Further study of this result shows that talc powder has flake structure, large aspect ratio, and good interfacial compatibility with PP, which is conducive to phonon heat transfer. This study proves that the thermal conductivity of the composite is related to not only the thermal conductivity of the filler itself but also the shape and interface structure of the filler.

Inorganic fillers with high thermal conductivity, such as alumina, aluminum nitride, silicon carbide, boron nitride, and expanded graphite (EG), can improve the thermal conductivity of composites in polymers while retaining the high insulation properties of materials (10–12). Alumina has excellent physicochemical properties, such as high temperature resistance, strong insulation, corrosion resistance, high thermal conductivity, and high strength. It can play an auxiliary role when two-dimensional fillers are connected to a thermal conduction network, which helps reduce anisotropy and is of low price. Therefore, it is widely used in ceramics, medicine, microelectronics, electrical machinery, and other industries. Compared with ordinary graphite, EG has a series of advantages: good chemical stability, low density, softness, and easy processing (13). In addition, its surface has a rich honeycomb pore structure to absorb other substances, so as to form a two-dimensional network heat conduction path and realize rapid heat transfer. EG has many excellent characteristics, is of low cost, and easy to manufacture, and so it is often used as a functional reinforcing filler to composite with other materials (11,12). The thermal conductivity of polymer materials is generally poor, whereas EG has good thermal conductivity and good compatibility with organic matter. It can be evenly dispersed in the matrix material with less addition, so as to significantly improve the thermal conductivity of polymer materials. Heat conductivity fillers have different shapes. the alumina mentioned above is granular and EG is flake, and this kind of multi-shape matching filler is easier to form heat conductivity path (14–16).

According to the research results of thermal conductivity and insulation properties and physical and mechanical properties of the composites filled with hybrid filler system, the prepared composites have better thermal conductivity and insulation properties only when the content of hybrid filler exceeds 50 wt% (17–19). However, at this time, the physical and mechanical properties of the composites will be significantly reduced, so that they cannot meet the requirements of some applications. Therefore, in the design of thermal conductive and insulating composites, we should consider not only the thermal conductive and insulating properties of the materials but also how to maintain good mechanical properties, especially the toughness of the materials. The toughening methods of PP include copolymerization modification, blending modification, and filling modification. Silane coupling agent has excellent chemical stability and is often used as a compatible modification component of plastics. The method of modifying PP with a silane coupling agent is simple and easy and is widely used at present. There are many kinds of silane coupling agents, and different silane coupling agents have different modification effects (20,21). Phenyltrimethoxysilane coupling agent (A153) has excellent chemical stability and high boiling point, which can meet the needs of PP processing.

In this study, PP with high temperature resistance was used as the basic material, and alumina powder (Al_2O_3) and EG PP/Al_2O_3/EG composite with better thermal conductivity and insulation and low cost were chosen as the research objects. In order to overcome the processing difficulties, poor mechanical properties, and weak electrical properties of high-filled polypropylene (PP) composites, A153 was used as the modified component of the composite system, and the effects of A153 content on the mechanical properties, thermal conductivity and insulation properties, and processability of PP thermal conductivity composite were discussed, which will provide a reference for practical application.

2 Experimental

2.1 Materials and instruments

PP, whose brand name is T30s, was purchased from Mitsui chemical company in Japan, and its physical parameters are shown in Table 1. Phenyltrimethoxysilane coupling agent (A153) was purchased from Shanghai Zhanyun Chemical Co., Ltd, whose molecular formula is shown in Figure 1a. Alumina powder (Al_2O_3), with an average size of about 1 μm as can be seen in Figure 1b, was obtained from Dongguan Dongchao New Material Technology Co., Ltd. EG, with the average size of about 20 μm as can be seen in Figure 1c, was supplied by Qingdao Yanhai carbon material Co., Ltd.

2.2 Sample preparation

In order to prepare ultra-high filling and ultra-high thermal conductivity PP composites, we designed relevant formulas (Table A1 in Appendix) and carried out pre-experiments.

Table 1: Physical parameters of pure PP

Physical parameters	PP
MFR ($g \cdot min^{-1}$)	2.3–3.7
Tensile strength (MPa)	≥29
Aggregate ash (%)	≤0.03
Isotactic index (%)	≥96

Table 2: Formula

Sample code	PP (phr)	EG (phr)	Al_2O_3 (phr)	A153 (phr)
PP-1	40	10	290	0
PP-2	40	10	290	2.5
PP-3	40	10	290	7.5
PP-4	40	10	290	12.5
PP-5	40	10	290	17.5

The results of the thermal conductivity experiment depicted in Figure A1 (in Appendix) show that when 10 parts of EG and 290 parts of Al_2O_3 are added to 40 parts of PP, the thermal conductivity of PP composites can reach up to 1.75 $W \cdot m^{-1} \cdot K^{-1}$, which is increased by 600% compared with pure PP. Therefore, this proportion is selected as the ratio for subsequent research. At the same time, we also tested the prepared PP composites by X-ray diffraction (XRD) and FTIR (Figures A2 and A3). The results show that no new impurities or other compounds are introduced in the processing process, which further proves that this ratio can produce good synergistic thermal conductivity. The composite materials were prepared by blending 40 phr PP (phr = parts per hundred), 10 phr EG, and 290 phr Al_2O_3 with different amounts of A153 by using an internal mixer with 60 rpm^{-1} and 190°C for 8 min (22,23). Afterward, the composite materials were kept under conditions of 15 MPa and 190°C for 5 min to form the plane sheets in the tablet press (yst-100t; Dongguan Tin Testing Instrument Co., Ltd). Details of the compositions in this work are listed in Table 2.

2.3 Characterizations

2.3.1 Mechanical properties

Put the dumbbell type sample on the electronic universal testing machine (ETM-A; Shenzhen Wance Testing Equipment Co., Ltd) and test it according to GB/T 1040-1992. The rate is 50 $mm \cdot min^{-1}$. Test each sample five times and take the average value.

2.3.2 Melt flow rate (MFR)

Measure the mass of the sample melt flowing out of the die with the specified diameter within 10 min at 230°C and 21.6 kg in a melt index meter (SRZ-400E; Shenzhen Wance Test Equipment Co., Ltd).

2.3.3 Volume resistivity

Test according to GB/T 1410-2006 in a high resistance meter (ZC-36 type; Shanghai Qiangjia Electric Co., Ltd).

2.3.4 Fourier transform infrared spectroscopy

The test conditions are as follows: resolution, 4 cm^{-1}; scanning times, 32 times; and scanning range, 3,500–700 cm^{-1} in a Fourier infrared spectrometer (TENSOR II, Brooke, Germany).

2.3.5 Thermal conductivity

Thermal conductivity was determined according to ISO 8301 in an LFA 1000 XFA500 (Linseis, Germany) with dry N_2 flowing at a rate of 20 $mL \cdot min^{-1}$.

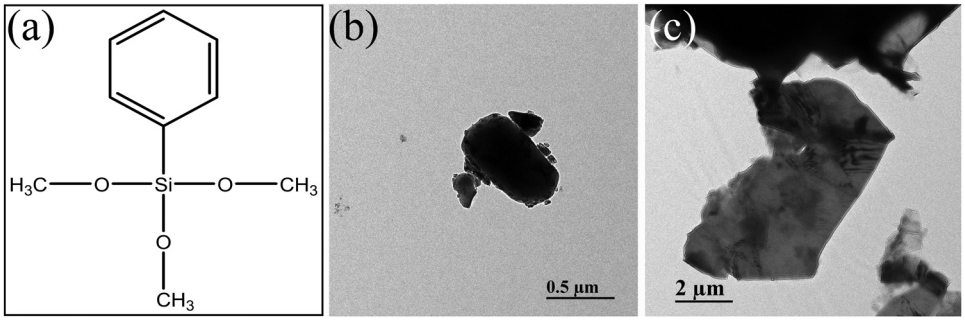

Figure 1: Molecular structure formula of A153 (a); the TEM diagrams of Al_2O_3 (b), and EG (c).

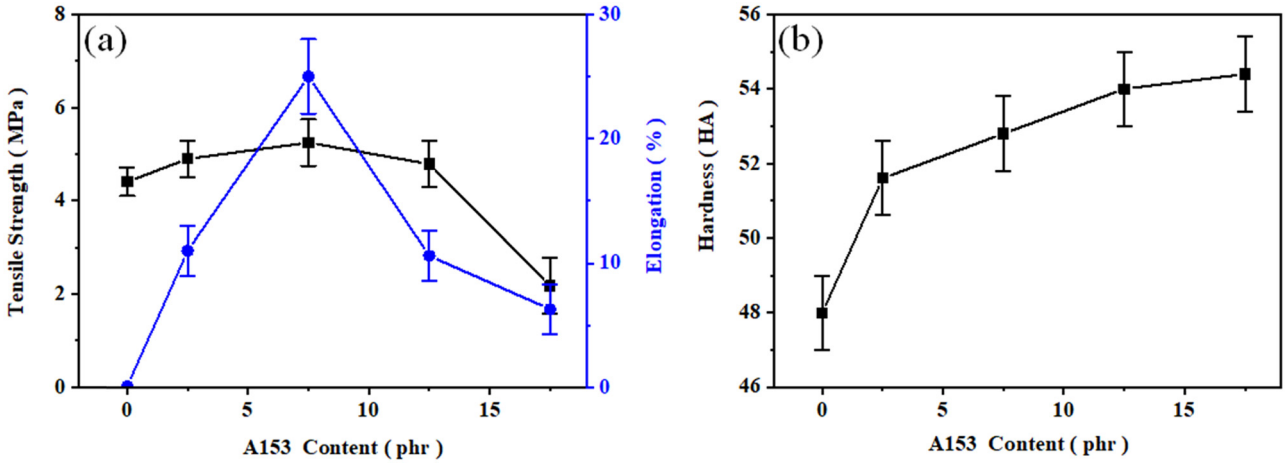

Figure 2: Effect of different content of A153 on mechanical properties of PP composites: (a) elongation at break and tensile strength and (b) hardness.

2.3.6 Rheological properties

The rotational speed of torque rheometer is 70 rpm and the processing temperature is 180–200°C in a torque rheometer (RM-200A; Harbin Hapu Electric Technology Co., Ltd).

2.3.7 Scanning electron microscopy (SEM)

The surface of the sample was sprayed with gold and then observed under the scanning electron microscope (Phenom Pro, Phenom-World B.V., the Netherlands) (12,13,24,25).

2.3.8 Dielectric strength

Place the sample on the dielectric strength tester and test it according to GB/T 1408.1-2006 in a dielectric mass spectrometer (IDAX300, Megger Company).

2.3.9 XRD

The crystal structures of the PP composites were characterized by XRD, which was performed with a rotating anode X-ray diffractometer (Japan Rigaku D/Max-Ra, Tokyo, Japan) equipped with a Cu Kα (λ = 0.1542 nm) radiation at 2θ values ranging from 5° to 60°.

3 Results and discussion

3.1 Mechanical properties

Figure 2a is a graph showing the change of elongation at break and breaking strength with A153 content. It can be seen from Figure 2a that when A153 is not added, the elongation at break of PP sample is almost 0%. With the increase of A153 addition, the elongation at break of PP sample first increases and then decreases. The elongation at break reaches its maximum when A153 addition is 7.5 phr and then continues to add A153, and the elongation at break begins to decrease. The breaking strength increases slightly with the increase in the amount of A153. When the amount of A153 is 7.5 phr, it reaches its maximum value, and if it continues to increase, then the strength decreases. This may be because A153 can promote the combination of EG particles and PP material surface, and a small amount of addition will significantly improve its tensile strength (26,27). When the amount of A153 is greater than 7.5 phr, excessive A153 begins to agglomerate, hindering the transmission of force and reducing the strength. The intermolecular elongation of A153 is also reduced. As an auxiliary agent with organic–inorganic hybrid structure, the silane coupling agent can improve the interfacial compatibility between PP and inorganic fillers, play the role of building a bridge, facilitate the transfer of force, and improve the mechanical properties in the macro.

Figure 2b is a graph showing the variation of shore A hardness with A153 content. As can be seen from Figure 2b, it increases with the increase of the addition amount of A153, but the increasing trend slows down when the addition amount of A153 exceeds 2.5 phr, which shows that a small amount of A153 can effectively improve the interfacial compatibility between PP and thermal conductivity additives and improve the properties of PP composites, while the influence of excessive A153 on it decreases gradually, so the changing trend of hardness slows down obviously (28).

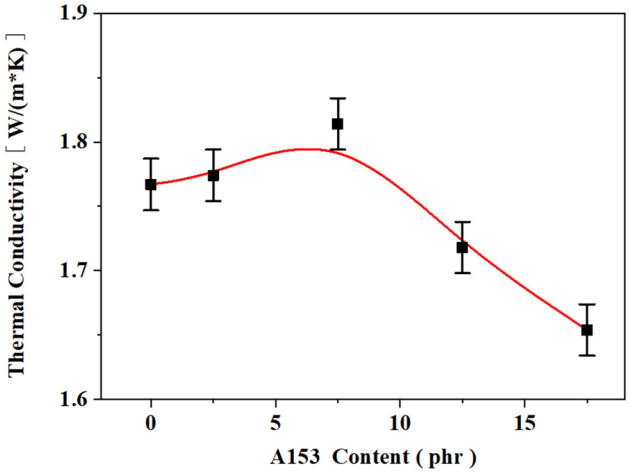

Figure 3: Effect of A153 content on thermal conductivity of PP composites.

3.2 Thermal conductivity

Figure 3 is a graph showing the variation of thermal conductivity with A153 content. It can be seen from Figure 3 that the measured thermal conductivity of the sample is between 1.65 and 1.82 $W \cdot m^{-1} \cdot K^{-1}$, which first increases slowly and then decreases with the increase of A153 addition. This may be because when A153 is introduced to a low content, A153 improves the bonding degree between continuous phase PP resin and inorganic particles in the composite, which then improves the interfacial compatibility between polymer and inorganic powder. At this stage, the heat conduction medium is mainly polymer resin matrix and powder complex (29,30). With the increase in the introduction amount of A153, a transition layer of A153 is gradually formed between the polymer matrix and the inorganic powder, which hinders the heat transfer between the powder and the polymer matrix. Although, due to the good thermal conductivity of the powder itself, the stable thermal conductivity channel can be formed between each other and occupies a dominant position in the influence on the thermal conductivity, the influence of the addition amount of A153 on the thermal conductivity is not obvious.

3.3 Volume resistivity

Figure 4 shows the curve of volume resistivity with A153 content. As can be seen from the figure, the volume resistivity first increases and then decreases with the increase of A153 addition. A small amount of A153 will significantly improve the volume resistivity of the sample, which shows that A153 in the material will significantly improve the insulation performance of the material. When the addition amount of A153 exceeds 7.5 phr, continue to increase A153, and the volume resistivity of the sample begins to decrease slowly (31,32). This may be because excessive addition of A153 will lead to molecular aggregation of A153, which will affect the overall volume resistivity of the material. When insulating materials are used in various parts of the electrical system, it is generally expected that the materials have as high insulation resistance as possible, and the appropriate addition of A153 can enhance the mechanical properties of the materials and improve the insulation properties of PP composites at the same time (33).

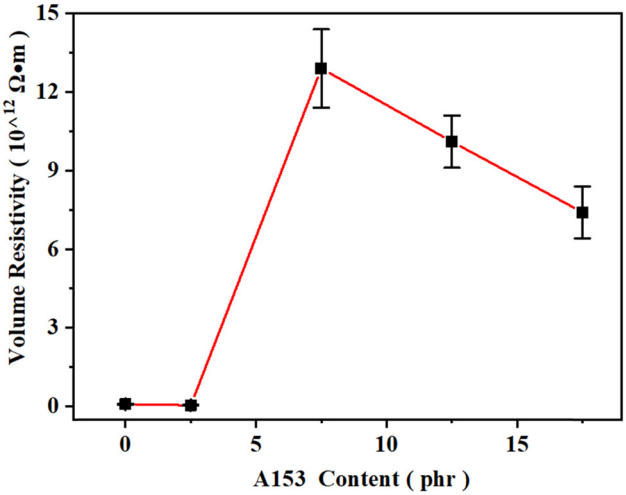

Figure 4: Effect of A153 content on volume resistivity of PP composites.

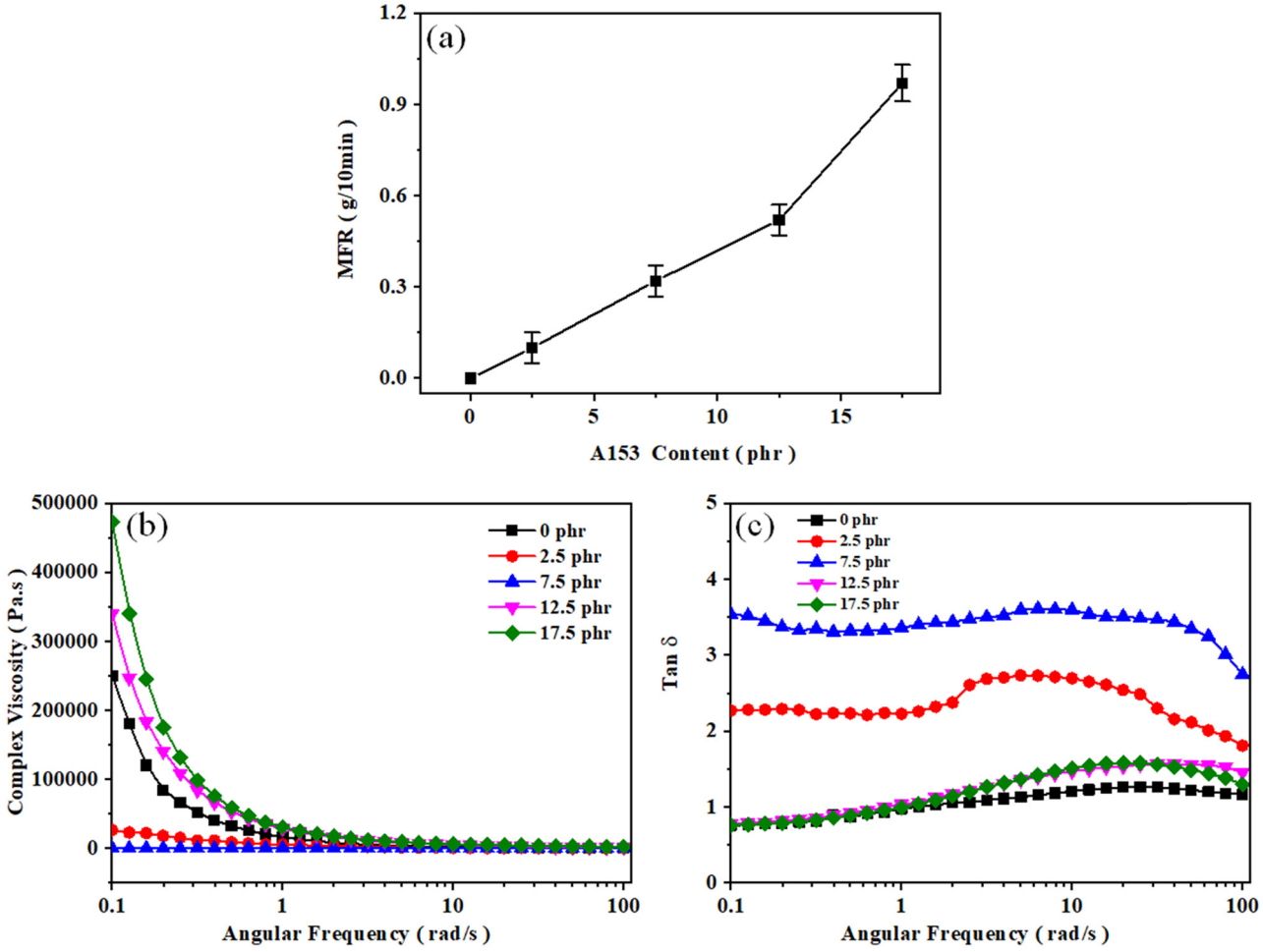

Figure 5: Effect of A153 content on processability of PP composites: (a) MFR, (b) viscosity, and (c) dielectric loss.

3.4 Processing performance

In order to study the effect of A153 on the processability of thermally conductive PP materials, MFR and rheological properties were tested, respectively. Figure 5a shows the variation curve of MFR with A153 content. It can be seen from Figure 5a that MFR increases with the increase of A153 content, from 0 to 0.9 g/10 min, which shows that A153 has a lubrication function and effectively reduces the huge friction resistance between PP and inorganic powder particles, so that PP composites can flow more easily in the melting process and are not prone to the sudden increase of torque (34). The higher the content of A153 in PP composites, the lower the friction resistance and the higher the MFR. The increase of MFR means that the energy consumption in industrial extrusion and molding process is reduced and the production efficiency is improved, which means that the addition of A153 makes PP composites show advantages in processing energy consumption and cost.

The viscosity curve in Figure 5b first decreases and then increases at low speed, because the addition of A153 hinders the relative fluidity between PP molecular chains and reduces the melt flow performance. At the same time, it can also be seen that the melt shear viscosity of PP blend decreases rapidly with the increase of shear rate and then gradually becomes slow (35). This is because, with the further increase of the shear rate, the conformation of the molecular chain changes from slow to fast, and the long-chain macromolecules deviate from the equilibrium conformation. Under the action of a high shear rate, the orientation of PP molecular chain reaches the limit state. At the same time, higher shear rate will break the melt and destroy the polymer structure. Therefore, when blending and melting, it is very important to select an appropriate melt shear rate to ensure the stable flow of the melt in the processing process.

Figure 5c shows the dielectric loss curve of samples with different A153 content. In the curve, there is a less obvious peak at 2.5 phr after the addition of component

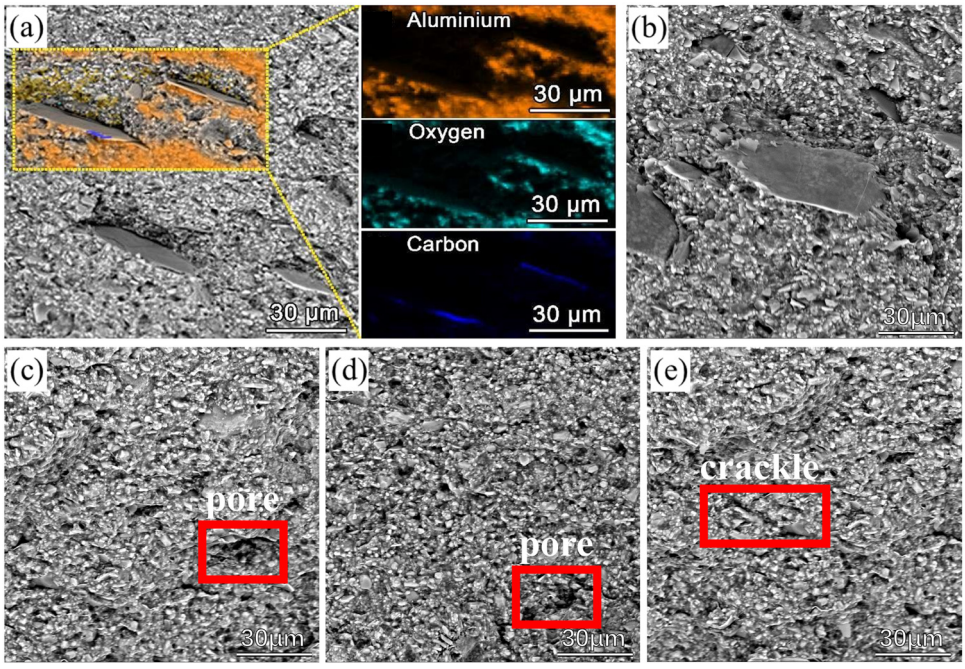

Figure 6: SEM cross section of PP samples with different A153 content: (a) PP-1, (b) PP-2, (c) PP-3, (d) PP-4, and (e) PP-5.

A153, which may be caused by the relaxation of ordered structure in the system after the addition of two-dimensional filler graphite (36). From the full frequency range, the curve of tan δ first increased and then decreased with the increase of A153 content. This is because the addition of A153 makes the whole system form a micro-order (37). However, when the content of A153 is greater than 7.5 phr, this micro-order is broken and tan δ decreases.

3.5 SEM

Figure 6 shows the cross-sectional morphology of PP samples with different A153 content. It can be seen from the figure that the section without A153 sample is relatively loose and has more pores. With the increase of A153 content, the structure of the sample gradually becomes compact and the pores gradually decrease (38,39). This shows that the proper addition of A153 can improve the interfacial compatibility between EG and PP, and the incompatible two materials are adsorbed by the organic–inorganic structure contained in A153, so as to reduce the internal cracks of PP composites. Therefore, its mechanical properties and processing properties are improved macroscopically. In addition, when the content of A153 exceeds 9 phr, the agglomeration phenomenon of alumina gradually appears, and cracks appear. This may be because too much A153 covers the inorganic filler, which makes the agglomeration phenomenon obvious, while the bonding between aggregates is weakened and cracks appear, thus affecting the properties of PP composites.

4 Conclusion

In order to improve the properties of high-filled thermal insulation PP composites, coupling agent A153 was used to modify it, and the effect of the number of A153 on PP composites was explored. The results of mechanical properties and insulation properties show that when the content of A153 reaches 7.5 phr, the tensile strength of PP composite can reach 5 MPa, the elongation at break can reach 25%, and the volume resistivity can reach 12.8×10^{12} Ω·m. Continuous addition of A153 will gradually increase the hardness, but the increase range decreases. The test results of thermal conductivity show that with the continuous addition of A153, the thermal conductivity first increases slowly and then decreases, and the maximum is $1.82\ W{\cdot}m^{-1}{\cdot}K^{-1}$ after the addition number reaches 7.5 phr. The results of the processing properties showed that with the increase of A153 content, MFR increased, the viscosity of PP composite decreased first and then increased at low speed, and the melt shear viscosity decreased rapidly and then gradually became slow with the increase of shear rate. The SEM results show that the

pore structure of A153 gradually decreases as the A153 content increases.

Acknowledgments: We are grateful to the Collaborative Innovation Center of Radiological Medicine of Jiangsu Higher Education Institutions.

Funding information: Financial support from Nuclear Energy Development and Scientific Research Project of the State Administration of Science, Technology and Industry for National Defense, P.R. China (No. 2019-1342) and Jiangsu Natural Science Foundation (No. BK20211318) is highly appreciated.

Author contributions: Jianxi Li: writing – original draft, data curation; Shuya Zhang: writing – review and editing, methodology; Yaqin Fan: data curation, formal analysis; Aosong Wang: project administration, funding acquisition; Zhuang Miao: investigation, formal analysis; Peng Cheng: validation; Hanzhou Liu: conceptualization, funding acquisition, writing – review and editing, methodology.

Conflict of interest: Authors state no conflict of interest.

Data availability statement: All data generated or analyzed during this study are included in this published article.

References

(1) Al Imran K, Lou J, Shivakumar KN. Enhancement of electrical and thermal conductivity of polypropylene by graphene nanoplatelets. J Appl Polym Sci. 2018;135(9):45833.
(2) Ahmadi M, Rouhi S, Ansari R. Evaluating the thermal conductivity coefficient of polypropylene/graphene nanocomposites: A hierarchical investigation. Proc Inst Mech Eng Part L-J Mater-Design Appl. 2021;235(12):2762–70.
(3) Du BX, Cui B. Effects of thermal conductivity on dielectric breakdown of micro, nano sized BN filled polypropylene composites. IEEE Trans Dielectr Electr Insulation. 2016;23(4):2116–25.
(4) Batool F, Bindiganavile V. Evaluation of thermal conductivity of cement-based foam reinforced with polypropylene fibers. Mater Struct. 2020;53(1):13.
(5) Atagur M, Akyuz O, Sever K, Seki Y, Seydibeyoglu O, Isbilir A, et al. Investigation of thermal and mechanical properties of synthetic graphite and recycled carbon fiber filled polypropylene composites. Mater Res Express. 2019;6(6):065312.
(6) Du H, Wu J, Liu G, Wu H, Yan R. Detection of thermophysical properties for high strength concrete after exposure to high temperature. J Wuhan Univ Technol-Mater Sci Ed. 2017;32(1):113–20.
(7) Fukuyama Y, Senda M, Kawai T, Kuroda S, Toyonaga M, Taniike T, et al. The effect of the addition of polypropylene-grafted SiO_2 nanoparticle on the thermal conductivity of isotactic polypropylene. J Therm Anal Calorim. 2014;117(3):1397–405.
(8) Ebadi-Dehaghani H, Reiszadeh M, Chavoshi A, Nazempour M, Vakili MH. The effect of zinc oxide and calcium carbonate nanoparticles on the thermal conductivity of polypropylene. J Macromol Sci Part B-Physics. 2014;53(1):93–107.
(9) Weidenfeller B, Kirchberg S. Thermal and mechanical properties of polypropylene-iron-diamond composites. Compos Part B-Engineering. 2016;92:133–41.
(10) King JA, Lopez Gaxiola D, Johnson BA, Keith JM. Thermal conductivity of carbon-filled polypropylene-based resins. J Composite Mater. 2010;44(7):839–55.
(11) Liu J, Shen L, Lin H, Huang Z, Hong H, Chen C. Preparation of Ni@UiO-66 incorporated polyethersulfone (PES) membrane by magnetic field assisted strategy to improve permeability and photocatalytic self-cleaning ability. J Colloid Interface Sci. 2022;618:483–95.
(12) Liu Y, Shen L, Huang Z, Liu J, Xu Y, Li R, et al. A novel in-situ micro-aeration functional membrane with excellent decoloration efficiency and antifouling performance. J Membr Sci. 2022;641:119925.
(13) Han L, Chen C, Shen L, Lin H, Li B, Huang Z, et al. Novel membranes with extremely high permeability fabricated by 3D printing and nickel coating for oil/water separation. J Mater Chem A. 2022;10:12055–61.
(14) Nejad SJ, Golzary A. Investigation and modeling of the thermal conductivity of PP/clay nanocomposites and PP/MWCNT nanocomposites. E-Polymers. 2010;94(1). doi: 10.1515/epoly.2010.10.1.1062.
(15) Muratov DS, Kuznetsov DV, Il'inykh IA, Mazov IN, Stepashkin AA, Tcherdyntsev VV. Thermal conductivity of polypropylene filled with inorganic particles. J Alloy Compd. 2014;586:S451–4.
(16) Liang J-Z. Estimation of thermal conductivity for polypropylene/hollow glass bead composites. Compos Part B-Eng. 2014;56:431–4.
(17) Roh JU, Kim HS, Lee WI. Isotropic conductivities in chopped carbon fiber composites using expanded polypropylene. Adv Composite Mater. 2014;23(5–6):409–20.
(18) Prakash V, Rai B, Tyagi VK, Niyogi UK. Dispersion and characterizations of nanofluids prepared with CuO and CNT nanoparticle. J Indian Chem Soc. 2015;92(8):1245–51.
(19) Pehlivanli ZO. Manufacturing and characterization of polypropylene/boric acid composite. Polym Bull. 2021;78(7):4033–46.
(20) Wang J-L, Xiong G-P, Gu M, Zhang X, Liang J. A study on the thermal conductivity of multiwalled carbon nanotube/polypropylene composite. Acta Phys Sin. 2009;58(7):4536–41.
(21) Vakili MH, Ebadi-Dehaghani H, Haghshenas-Fard M. Crystallization and thermal conductivity of $CaCO_3$ nanoparticle filled polypropylene. J Macromol Sci Part B-Physics. 2011;50(8):1637–45.
(22) Xu S, Zhou C, Li J, Shen L, Lin H. Simultaneously improving mechanical strength, hydrophobic property and flame retardancy of ethylene vinyl acetate copolymer/intumescent flame

retardant/FeOOH by introducing modified fumed silica. Mater Today Commun. 2021;26:26.
(23) Xu S, Li J, Ye Q, Shen L, Lin H. Flame-retardant ethylene vinyl acetate composite materials by combining additions of aluminum hydroxide and melamine cyanurate: Preparation and characteristic evaluations. J Colloid Interface Sci. 2021;589:525–31.
(24) Huang Z, Zeng Q, Liu Y, Xu Y, Li R, Hong H, et al. Facile synthesis of 2D TiO_2@MXene composite membrane with enhanced separation and antifouling performance. J Membr Sci. 2021;640:640.
(25) Chen B, Xie H, Shen L, Xu Y, Zhang M, Yu H, et al. Electroless Ni-Sn-P plating to fabricate nickel alloy coated polypropylene membrane with enhanced performance. J Membr Sci. 2021;18:640.
(26) Chauhan SS, Aggarwal P, Karmarkar A. The effectiveness of m-TMI-grafted-PP as a coupling agent for wood polymer composites. J Composite Mater. 2016;50(25):3515–24.
(27) Aggarwal PK, Raghu N, Karmarkar A, Chuahan S. Jute-polypropylene composites using m-TMI-grafted-polypropylene as a coupling agent. Mater & Des. 2013;43:112–7.
(28) Das K, Ray D, Adhikary K, Bandyopadhyay NR, Mohanty AK, Misra M. Development of recycled polypropylene matrix composites reinforced with fly ash. J Reinforced Plast Compos. 2010;29(4):510–7.
(29) Deng S, Beehag A, Hillier W, Zhang D, Ye L. Kenaf-polypropylene composites manufactured from blended fiber mats. J Reinforced Plast Compos. 2013;32(16):1198–210.
(30) de la Orden MU, Gonzalez Sanchez C, Gonzalez Quesada M, Martinez Urreaga J. Effect of different coupling agents on the browning of cellulose-polypropylene composites during melt processing. Polym Degrad Stab. 2010;95(2):201–6.
(31) Madhavi S, Raju NV, Johns J. Characterization of bamboo – polypropylene composites: effect of coupling agent. Fibers Polym. 2021;22(11):3183–91.
(32) Lee M, Kim Y, Ryu H, Baeck S-H, Shim S. Effects of silane coupling agent on the mechanical and thermal properties of silica/polypropylene composites. Polymer-Korea. 2017;41(4):599–609.
(33) Miyazaki K, Okazaki N, Terano M, Nakatani H. Preparation and characterization of cellulose/polypropylene composite using an oxidatively degraded polypropylene. J Polym Environ. 2008;16(4):267–75.
(34) Ndiaye D, Tidjani A. Effects of coupling agents on thermal behavior and mechanical properties of wood flour/polypropylene composites. J Composite Mater. 2012;46(24):3067–75.
(35) Nourbakhsh A, Ashori A. Highly fiber-loaded composites: Physical and mechanical properties. Polym & Polym Compos. 2008;16(5):343–7.
(36) Subramaniam D, Natesan R, Shanmugavel BP. Development of storage bin using lantana camara flour reinforced polypropylene composites: Product performance study on the composite bin for pharmaceutical applications. J Polym Res. 2022;29(4):122.
(37) Poletto M. Natural oils as coupling agents in recycled polypropylene wood flour composites: Mechanical, thermal and morphological properties. Polym Polym Compos. 2020;28(7):443–50.
(38) Wang Y, Cao J, Zhu L, Zhao G. Interfacial compatibility of wood flour/polypropylene composites by stress relaxation method. J Appl Polym Sci. 2012;126:E89–95.
(39) Vantsi O, Karki T. Different coupling agents in wood-polypropylene composites containing recycled mineral wool: A comparison of the effects. J Reinforced Plast Compos. 2015;34(11):879–95.

Appendix

Table A1: Pre-experimental formula

Code	PP (phr)	EG (phr)	Al_2O_3 (phr)
PP-1	40	0	200
PP-2	40	0	300
PP-3	40	5	295
PP-4	40	10	290
PP-5	40	15	285

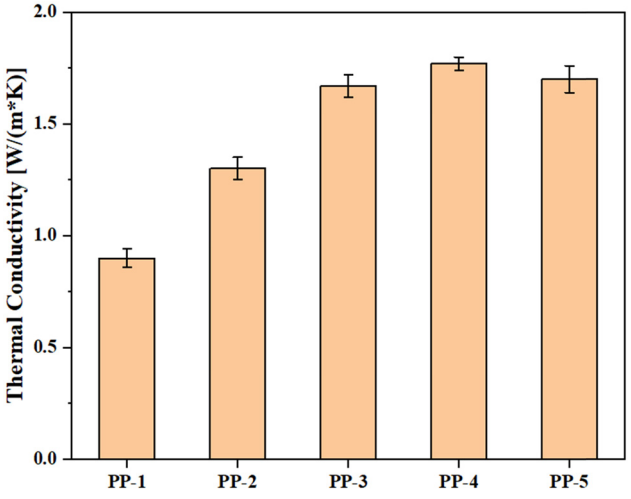

Figure A1: Effect of different EG and Al_2O_3 ratios on thermal conductivity of PP composites.

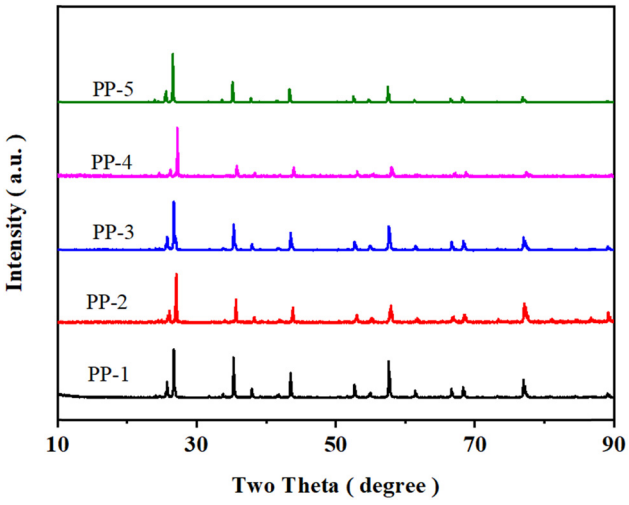

Figure A2: Effect of different EG and Al_2O_3 ratios on XRD of PP composites.

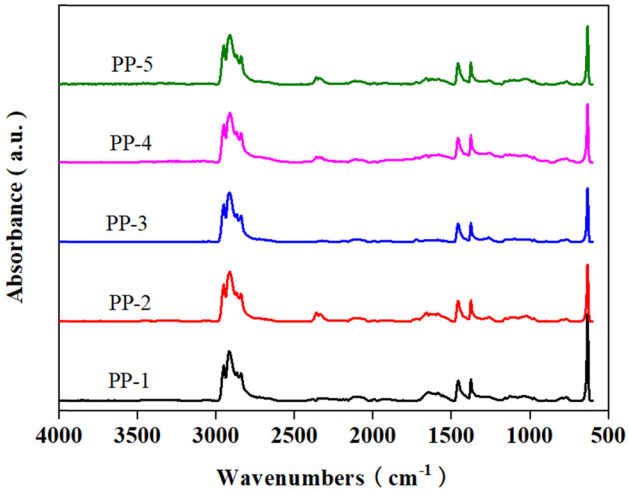

Figure A3: Effect of different EG and Al_2O_3 ratios on FTIR of PP composites.